

# Derivation of the Distributions of Long Chain Branching, Molecular Weight, Seniority, and Priority for Polyolefins Made with Two Metallocene Catalysts

Daniel J. Read<sup>\*,†</sup> and Joao B. P. Soares<sup>‡</sup>

Department of Applied Mathematics, University of Leeds, Leeds, LS2 9JT, U.K., and  
Institute for Polymer Research, Department of Chemical Engineering, University of Waterloo,  
200 University Avenue West, Waterloo, Ontario, Canada N2L 3G1

Received June 24, 2003; Revised Manuscript Received October 13, 2003

**ABSTRACT:** We obtained the molecular weight and long chain branching distribution for polyolefins made with a combination of two single-site metallocene catalysts in a CSTR. Long chain branches are assumed to be formed by the incorporation of chains formed with a double bond end (macromers) at the catalyst sites. In the case where one of the catalysts produces only linear chains, we obtain explicit expressions for both the bivariate molecular weight and branching distribution, and the overall molecular weight distribution. In the general case where both catalysts incorporate branches, we are unable to obtain an explicit expression, but we can define a recursive algorithm which rapidly gives exact results for these two distributions. We compare the distributions with results from a more conventional population balance on the same system. We also obtain recursive algorithms for the statistical distribution of the topological variables seniority and priority for this general case, illustrating how they change with the reactor variables.

## 1. Introduction

Metallocene catalysts that produce polyolefins with long chain branches (LCB) have considerable industrial interest. These catalysts produce polyolefins with narrow molecular weight distributions and an amount of LCB typically varying from 0.1 to 1 LCB per 1000 carbon atoms. Remarkably, the presence of even a few LCB can significantly affect the rheological and physical properties of these polymers, leading to resins with enhanced performance.

Constrained geometry catalysts are commonly used to produce polyethylene with LCB.<sup>1–3</sup> However, LCB formation is not limited to this class of monocyclopentadienyl catalysts; several other metallocene types have been used to synthesize polyolefins with LCBs,<sup>4,5</sup> including the incorporation of LCB with different chemical structures from the backbone.<sup>6–9</sup> LCB formation with different metallocenes has been observed in solution, slurry, and gas-phase reactors.

Regardless of the type of catalyst and reactor configuration, the mechanism of branch formation with metallocenes is terminal branching: dead chains containing terminal unsaturations (preferably vinyl) copolymerize with growing chains to form branches with the length of the dead chains (minus two carbon atoms). These dead chains with terminal unsaturations are usually called *macromonomers*. Therefore, LCB formation with metallocenes is simply copolymerization with a long comonomer chain and thus it should be expected that catalysts that have high reactivity ratios toward long  $\alpha$ -olefins can also produce polyolefins with LCB. This is indeed the case, as shown in several experimental investigations.<sup>1–9</sup>

Preformed macromonomer may be added to the polymerization reactor, in which case these polymeriza-

tions can be treated as common copolymerizations, or macromonomer may be formed in situ by the same catalyst, making the branched chains, or by a second catalyst added for this specific purpose. In situ formation of polyethylene macromonomers happens when living polyethylene chains are terminated via  $\beta$ -hydride elimination or transfer to ethylene. (A few other mechanisms can lead to macromonomer formation during propylene polymerization.<sup>6</sup>) If the latter mechanism of LCB formation is predominant, the polymers made with these catalysts have a complex LCB architecture composed of linear and branched chains, as described in detail in the literature.<sup>10</sup>

Soares and Hamielec<sup>11–13</sup> derived an analytical solution for the distribution of molecular weight, chemical composition and long chain branching for polymers made with a single metallocene catalyst. Different modeling approaches<sup>14–16</sup> confirmed the expression previously obtained by Soares and Hamielec and, in one case,<sup>15</sup> additionally derived the statistical distribution of other variables (seniority and priority) relevant to the melt rheology, which were dependent upon the polymer architecture. A more in-depth picture of the branching structure of these chains can be obtained via Monte Carlo models.<sup>16,17</sup> Taking this approach, Beigzadeh et al.<sup>17</sup> found that most of the high molecular weight chains had branches on branches. This is a very important observation, since these highly branched structures can enhance polymer processability considerably and may account for the excellent rheological properties of these resins.

For a given catalyst type, the LCB frequency of the resulting polymers can be enhanced by increasing the concentration of macromonomer present in the reactor. For solution polymerization there are essentially three ways of achieving this objective: (1) operate the reactor at high conversions, (2) feed preformed macromonomer to the reactor, and (3) add a second catalyst with a higher rate of macromonomer formation to the reactor.

<sup>†</sup> University of Leeds.

<sup>‡</sup> University of Waterloo.

Gas-phase polymerization has also been used to increase the concentration of macromonomers around the active sites,<sup>18</sup> but in this case bulk chain mobility is severely decreased. This might also lead to a different branching structure, with unknown consequences to polymer properties.

The use of a dual metallocene catalyst system was investigated by Beigzadeh et al.,<sup>19–21</sup> both theoretically and experimentally, confirming that LCB frequency can be enhanced if two adequate metallocenes are combined in the same reactor. However, as noticed by the same authors,<sup>10</sup> this LCB-enhancement process would affect the branching structure of the polymer since the proportion of chains with comb structures would be higher than that present when a single CGC catalyst was used. It is well-known that tree- and comb-branched polymers have quite different rheological behaviors. Therefore, the LCB enhancement obtained by combining two metallocene catalysts might affect the final rheological (and mechanical) properties of the polymer in a rather complex and so far unpredictable way.

Soares<sup>22</sup> developed a simple mathematical model to predict the branching density of polyolefins made with two metallocene catalysts, in which one metallocene makes only linear chains (linear catalyst) and the other produces linear and branched chains (LCB catalyst). This can be achieved in practice by combining two metallocenes with very different reactivity ratios toward  $\alpha$ -olefins. The most attractive feature of the model is that it is computationally simple and uses just a few dimensionless parameters that can be obtained via <sup>13</sup>C NMR analysis of chain ends and branch structure of polymers made with each metallocene catalysts separately. The model was used to investigate polymerization conditions and catalysts combinations that would maximize the formation of a given polymer population. It was shown that when the selectivity for macromonomer formation of the linear catalyst is the same as that of the LCB catalyst, it was not possible to maximize the number of LCB per chain, even though the number of LCB per 1000 carbon atoms could be maximized. On the other hand, if the selectivity for macromonomer formation of the linear catalyst was higher than that of the LCB catalyst, both LCB/1000 C and LCB/chain passed through maxima when varying the fraction of linear catalyst in the reactor. More importantly, each polymer population reaches its maximum value at a different ratio of linear catalyst to LCB catalyst, thus permitting the maximization of individual polymer populations in the mixture. Similar results were obtained via Monte Carlo simulation by Simon and Soares<sup>23</sup> in a more detailed paper that also included the prediction of complete molecular weight distributions. Very recently, a recursive algorithm was proposed by Costeux<sup>24</sup> which allowed the exact prediction of the probability distribution for number of branches on a chain and an approximate prediction for the molecular weight distribution for this same system. He also proposed a Monte Carlo algorithm for generating molecular architectures, for the dual catalyst system, as did Beigzadeh.<sup>25</sup> Iedema et al.<sup>26</sup> have developed a population-balance approach to this system, which gives predictions of the molecular weight distribution and an approximate branching distribution, but no detailed information on the molecular architecture.

In this paper, we develop an analytical model to describe the exact distributions of molecular weight and

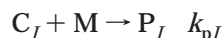
long chain branching for polymers made with two metallocene catalysts. We are able to obtain explicit analytical results for the case when one of the catalysts does not react with  $\alpha$ -olefins and produces linear chains only. We also present a recursive algorithm for the general case, similar in structure to that given by Costeux,<sup>24</sup> but which gives exact (rather than approximate) distributions. In both cases, we verify the results by comparison against a more conventional "population balance"<sup>12,26</sup> approach to obtaining these distributions numerically.

The use of combined metallocene catalysts is potentially very important because it permits the production of polyolefins with the unique microstructures described in the several references mentioned above. One way of quantifying the differences between these microstructures is via the topological variables *seniority* and *priority* described in ref 15. We shall generalize the methodology developed in that paper to obtain the statistical distribution of these two variables for a mixed metallocene ensemble. It is our hope that the analytical solutions and numerical algorithms presented here may help select adequate catalysts for the synthesis of polyolefins with designed molecular weight and long chain branch distributions.

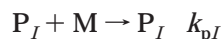
## 2. Reaction Chemistry

In this paper we use, and generalize the reaction chemistry described by Soares<sup>22</sup> for formation of long chain branched PE in a system with multiple metallocene catalysts. For each type of catalyst,  $I$ , there are a number of possible reactions that can occur. These are represented schematically as

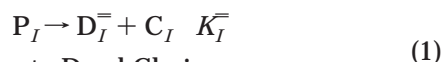
### 1. Initiation



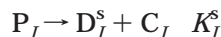
### 2. Monomer Addition



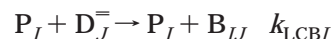
### 3. Chain Transfer to Double Bond



### 4. Chain Transfer to Dead Chain



### 5. Long-Chain Branch Formation



In the first reaction, a monomer ( $M$ ) is added to the catalyst site ( $C_I$ ), initiating the growth of a "living" chain ( $P_I$ ). During the subsequent monomer addition (reaction 2) the resulting chain remains attached to the catalyst, and so retains the label  $P_I$  for a living chain (we can add further subscripts later, as is done in Appendix B where the full population balance equations are given).

In the third reaction, the living chain detaches from the catalyst site so that it now terminates with a double bond (denoted by  $D_I^-$ )—i.e., it becomes a "macromonomer". This process can occur either by  $\beta$ -hydride elimination or by transfer to monomer as described by Soares;<sup>22</sup> the rate constant  $K_I^-$  is the one appropriate for the sum of these two processes, and depends on the catalyst site. Such a detached chain may take part later

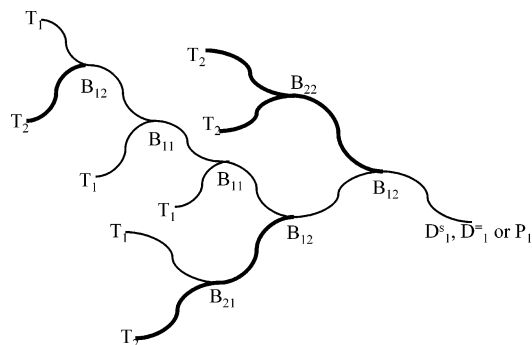


**Figure 1.** Schematic diagram of a branched molecule formed by a reaction involving two metallocene catalysts. Thin lines represent chain strands formed at catalyst 1, thick lines represent strands formed at catalyst 2. Also shown are initiation sites ( $T_1$  and  $T_2$ ) and branching sites ( $B_{11}$ ,  $B_{12}$ ,  $B_{22}$ , and  $B_{21}$ ). This particular molecule is a “catalyst 1” molecule—there are similarly shaped molecules which terminate in a  $P_2$ ,  $D_2^s$ , or  $D_2^-$  group. For all the strands, the direction in which they were polymerized (“downstream”) is left to right.

in LCB formation. We shall distinguish between chains detached from different catalyst sites (by using the subscript  $I$  in  $D_I^-$ ) because, although they are chemically identical, they are statistically different in terms of molecular weight and number of branches.

In the fourth reaction, a living chain detaches from the catalyst site, but without leaving a trailing double bond. The resulting dead chain ( $D_I^s$ ) plays no further part in the reaction. This reaction is usually prompted by a “chain transfer agent” such as hydrogen or aluminum; the rate constant  $K_I^s$  is the one appropriate for the sum over all chain transfer agents.

The final reaction gives rise to long chain branch formation: In this last reaction, a living chain ( $P_I$ ) reacts with a macromonomer ( $D_J^-$  where the subscript  $J$  denotes that the macromonomer might have detached from a different catalyst  $J$ ). The result is a living chain ( $P_I$ ) containing an extra branch point (labeled  $B_{IJ}$ ). The subscript  $IJ$  is used to distinguish between branches formed from reactions between the different macromonomer and living chain populations.

It is, additionally, possible for a macromonomer to react directly with an uninitiated branching catalyst site:



This reaction is relatively rare (compared to LCB formation) because, under typical reaction conditions, the concentration of uninitiated catalyst is much smaller than that of the living polymer. Inclusion of this reaction results in additional complications to the maths that follows (one needs to consider the points where a chain swaps between growth on different catalysts). Nevertheless, because it is a rare event, it will only produce a small correction to the results of this paper. For this reason, we omit this reaction from our present considerations. It is, however, effectively included in the full population balance equations given in Appendix B (where it is present in the “long chain branch” formation step), so that the two methods give very slightly different results.

**2.1. Qualitative Description of the Chain Structure.** From the reaction discussed above, it is clear that the chains formed have a typical shape, illustrated in Figure 1 for a two-catalyst system. Each chain contains

just one unique free end attached to either a catalyst site ( $P_I$  chains) a double bond ( $D_I^-$  chains) or a dead end ( $D_I^s$  chains). All other free ends in the molecule were produced in an initiation step. As described previously,<sup>15</sup> it is possible to define a direction on each polymer strand between cross-links, pointing along the molecule toward the unique free end (i.e., left to right in Figure 1). This is the direction in which monomers were added to the polymer molecule, the growth direction. This direction is preserved during all the above reactions, notably during the formation of long-chain branches (the directions of the arrows on the reacting  $P_I$  and a  $D_I^-$  species remain the same in the resulting  $P_I$  species). As before,<sup>15</sup> we call the molecular direction toward the unique free end *downstream* and the opposite direction *upstream*.

The new feature of the mixed metallocene system is the presence, in Figure 1, of different branch point “types”. These are sites at which  $D_J^-$  macromonomers from catalyst site  $J$  were incorporated into the growing chain  $P_I$  on catalyst site  $I$  (giving a branch point  $B_{IJ}$ ) where in the figure,  $I$  and  $J$  take the values 1 or 2. We also distinguish, in Figure 1, between chain sections which were polymerized at different sites. The molecular weight distributions of a strand depends on the catalyst site at which it was created, in general.

## 2.2. Detailed Balance in a Steady-State CSTR.

We now make the further assumption that the polymerization reaction is performed in a steady-state continuous stirred tank reactor (CSTR), which is typical for metallocene LCB polymerizations. In the idealization of this, it is assumed that the concentration of reagents varies neither in time nor space within the reaction vessel. This allows us to write down detailed balance equations for each reagent as follows.

We denote with a subscript the concentration of a specific fraction  $x$  of a species ( $x$  might be degree of polymerization or number of branch points). For example,  $P_{I,x}$  is the (number) concentration of  $P_I$  species with property  $x$ . The total concentration of a given species is denoted without a subscript, so (for example)  $P_I = \sum_x P_{I,x}$ . We can write detailed balance equations for the whole concentration of a species, or fraction by fraction.

From eq. 1, the rate equations for  $P_I$  and  $C_I$  are

$$\frac{dP_I}{dt} = -sP_I - K_I^s P_I - K_I^- P_I + k_{pI} M C_I \quad (3)$$

$$\frac{dC_I}{dt} = -sC_I + K_I^s P_I + K_I^- P_I - k_{pI} M C_I + \text{feed}_I \quad (4)$$

where  $s$  is the inverse of the mean residence time, and  $\text{feed}_I$  represents the input of catalyst into the reactor. Since we are in a steady state, the time derivatives may be set to zero, and we obtain two equations which are equivalent only if

$$\text{feed}_I = s(P_I + C_I) \quad (5)$$

In this steady-state condition,  $P_I$  and  $C_I$  are related by

$$C_I = \frac{P_I(s + K_I^s + K_I^-)}{k_{pI} M} \quad (6)$$

The rate equations for each fraction of the macromono-



mer and dead chain species are

$$\frac{dD_{I,x}^{\overline{\overline{}}}}{dt} = K_I^{\overline{\overline{}}} P_{I,x} - (s + h) D_{I,x}^{\overline{\overline{}}} \quad (7)$$

$$\frac{dD_{I,x}^s}{dt} = K_I^s P_{I,x} - s D_{I,x}^s \quad (8)$$

where

$$h = \sum_I k_{LCBI} P_I$$

Again setting time derivatives to zero, we obtain

$$D_{I,x}^{\overline{\overline{}}} = \frac{K_I^{\overline{\overline{}}} P_{I,x}}{s + h} \quad (9)$$

$$D_{I,x}^s = \frac{K_I^s P_{I,x}}{s} \quad (10)$$

These last two equations are true both fraction by fraction (i.e., with subscripts) and for the population of each species as a whole. It follows that the probability distribution of  $D_{I,x}^{\overline{\overline{}}}$  and  $D_{I,x}^s$  with respect to any variable,  $x$  (for example, the molecular weight distribution) is identical to that of the living polymers at site  $I$ ,  $P_{I,x}$ . As described previously,<sup>11–13,15,16</sup> the statistical distribution of the living, dead and double bond chain species are identical, but we must derive separate distributions for each site  $I$ .

We can also obtain an expression for the concentration of branch points,  $B_{IJ}$ , in the reactor vessel, which will be of use later. The rate equation is

$$\frac{dB_{IJ}}{dt} = k_{LCBI} P_I D_J^{\overline{\overline{}}} - s B_{IJ} \quad (11)$$

giving

$$B_{IJ} = \frac{k_{LCBI} P_I D_J^{\overline{\overline{}}}}{s} \quad (12)$$

at the steady state.

**2.3. Estimation of Kinetic Parameters.** From the above equations, it is clear that a number of kinetic parameters are required for any modeling of a reactor. For each catalyst, the required parameters are the four kinetic constants in eq. 1,  $k_{pI}$ ,  $K_I^{\overline{\overline{}}}$ ,  $K_I^s$ , and  $k_{LCBI}$  and the overall living chain concentration,  $P_I$ . Additionally, the mean residence time,  $1/s$ , and the monomer concentration,  $M$ , are reactor operational parameters set by reactor design and changed as needed during operation ( $M$  is a function of monomer partial pressure and solubility in the solvent used during polymerization).

The estimation of kinetic parameters for these metallocene systems in the presence of long chain branch formation has been the subject of recent investigations.<sup>22,27,28</sup> The next paragraphs summarize these previously published results. We will assume that each catalyst in the mixture acts independently of each other. Under this assumption, the polymerization kinetic constants can be obtained from separate experiments with each catalyst.

The parameter  $k_{pI}$  is estimated using standard polymer reaction engineering methods from the rate of polymerization.<sup>28</sup> The concentration of living polymer

in the reactor,  $P_I$  (which, for all practical purposes, is equal to the concentration of catalysts in the reactor, as  $C_I \ll P_I$ ), is known from the feed flow rate of catalyst to the CSTR, the rate of catalyst deactivation (not considered in the present model), and the average residence time in the reactor. A simple molar balance is required for this calculation.<sup>22</sup> The total concentration of dead chains in the reactor,  $D_I^{\overline{\overline{}}} + D_I^s$ , can be directly measured during polymerization. <sup>13</sup>C NMR can be used to determine the fraction of chains that have terminal saturations,  $x_I^s$ , and unsaturations,  $x_I^{\overline{\overline{}}}$ . Consequently:

$$D_I^s = x_I^s (D_I^{\overline{\overline{}}} + D_I^s)$$

$$D_I^{\overline{\overline{}}} = x_I^{\overline{\overline{}}} (D_I^{\overline{\overline{}}} + D_I^s)$$

Rates constants for long chain branch formation,  $k_{LCBI}$  can be calculated from total branching frequency ( $\lambda = \text{LCB}/1000 \text{ C}$ ) measured by <sup>13</sup>C NMR using the following equation, applicable in a single catalyst reactor:<sup>28</sup>

$$k_{LCBI} = \frac{\lambda}{500 - \lambda} \frac{k_{pI} M}{D_I^{\overline{\overline{}}}} \quad (13)$$

This provides sufficient information so that eqs 9 and 10 can be used to obtain  $K_I^{\overline{\overline{}}}$  and  $K_I^s$  for the given reactor conditions. Since  $K_I^{\overline{\overline{}}}$  includes a “transfer to monomer” process, it will depend on  $M$  (to first approximation, we would anticipate a linear dependence on  $M$ ). Similarly,  $K_I^s$  depends on the concentrations of different chain transfer agents (again we would anticipate a linear dependence). A number of experiments are required to confirm these anticipated linear relationships and obtain the coefficients so that  $K_I^{\overline{\overline{}}}$  and  $K_I^s$  can be estimated for all reactor conditions.

To further confirm the self-consistency of the obtained parameters, one could compare the molecular weight (and, possibly, branching) distribution with the predicted distribution for single-catalyst systems.<sup>11–13,14–16</sup> The model parameters can also be set up in such a way that they acquire physical meaning. For one such approach, the reader is referred to Soares;<sup>22</sup> a second such approach is given in section 3.1 below.

### 3. Derivation of Chain Statistics for Two Catalysts

The above equations are written for an arbitrary number of catalysts,  $I$ . In this section, we derive chain statistics for the case of just two catalysts. We shall obtain some explicit analytical results for the case where one catalyst does not form long chain branches ( $k_{LCB2} = 0$ ), and an implicit (but numerically very rapid) scheme for the general case where both catalysts form branches. We begin by defining the minimum parameter set for this latter case.

**3.1. Parameter Set.** In the above section we demonstrated that, separately for each type of catalyst in steady-state conditions, the statistical distribution of the living, dead and double bond polymer species were identical. We now consider the long-chain branching reactions. We note that a reaction forming a “ $B_{IJ}$ ” branch combines a  $P_I$  species and a  $D_J^{\overline{\overline{}}}$  species. These species are taken from statistical distributions that depend on the type of catalyst from which they originated. The resulting chain, a  $P_I$  species, must be part of that same (catalyst  $I$ ) statistical distribution. Hence,

the statistics of each of the sub-branches on a  $B_{IJ}$  branch point must have identical statistics to the whole chains on the catalysts from which they originated. These properties are true of every branch-forming reaction so, as for the single catalyst case,<sup>15</sup> the molecules are “self-similar” *provided one distinguishes between the different types of sub-branch according to their catalysts* (this is in contrast to the statement made by Iedema et al.<sup>25</sup> that the self-similarity is broken in multiple catalyst systems).

To calculate the molecular weight and branching distribution for this class of metallocene polymers, we shall make use of the self-similarity of the polymer chains, via branching probabilities as was done previously for the single metallocene case.<sup>15</sup> We define “upstream” branching probabilities, as follows. We focus on the polymer strands that were formed by polymerization on catalyst  $I$ . If we pick one of these polymer strands at random from the reaction mixture, then we define the probability of first hitting a branch point of type  $B_{IJ}$  by stepping along the chain in the upstream direction as  $b_{IJ}$  (and the probability of hitting a chain end is  $1 - \sum_J b_{IJ}$ ). Note that it is impossible to hit a branch point of type  $B_{12}$  going *upstream* from catalyst 2 strands because a  $B_{12}$  branch point incorporates a  $D_2^-$  chain into a polymerizing  $P_1$  chain. Similarly, one cannot hit a branch point of type  $B_{21}$  upstream from a strand of type 1.

The probabilities  $b_{IJ}$  may be calculated from the concentrations of reactive species derived above through the detailed balance equations, as follows. We note that, for any of the polymer chains in the reaction bath, there is a single free end with a double bond, dead end or catalyst attached. All other free ends were produced in initiation steps. We define “initiation” sites  $T_I$  for each catalyst  $I$ . A chain of type  $I$ , once initiated, will polymerize until it is detached from the site, forming a double bond  $D_I^-$  or a dead chain  $D_I^s$ . The double bond might be incorporated in another chain polymerizing on catalyst  $J$ , forming a branch point of type  $B_{JI}$ . Hence the total concentration of initiation sites of type  $I$  is simply

$$T_I = P_I + D_I^- + D_I^s + \sum_J B_{JI} \quad (14)$$

We also use the concentration  $S_I$  of strands of type  $I$ , which we obtain by counting the number of strands immediately upstream from either a branch point or chain end:

$$\begin{aligned} S_I &= P_I + D_I^- + D_I^s + \sum_J (B_{JI} + B_{IJ}) \\ &= 2B_{II} + B_{12} + B_{21} + P_I + D_I^- + D_I^s \end{aligned} \quad (15)$$

The upstream branching probability  $b_{11}$  is simply the total number of strands which hit a  $B_{11}$  branch point upstream, divided by the total number of catalyst 1 strands ( $S_1 = 2B_{11} + B_{12} + B_{21} + P_1 + D_1^- + D_1^s$ ).

$$b_{11} = \frac{B_{11}}{S_1} = \frac{B_{11}}{2B_{11} + B_{12} + B_{21} + P_1 + D_1^- + D_1^s} \quad (16)$$

In general,

$$b_{IJ} = \frac{B_{IJ}}{S_I} \quad (17)$$

where  $I$  and  $J$  take the values 1 or 2. These branching probabilities define the topology of the chains. It is clear, from the definitions above, that the following inequalities apply

$$\begin{aligned} 1 - 2b_{11} - b_{12} &> 0 \\ 1 - 2b_{22} - b_{21} &> 0 \\ (1 - 2b_{11} - b_{12})(1 - 2b_{22} - b_{21}) - b_{12}b_{21} &> 0 \end{aligned}$$

These set limits on the allowable values for the branching probabilities. Moreover,

$$\frac{b_{11}}{b_{12}} = \frac{b_{21}}{b_{22}} = \frac{D_1^-}{D_2^-} = \frac{K_1^- P_1}{K_2^- P_2} \quad (18)$$

which indicates that there are only three independent branching probabilities in the system.

In terms of the reactor variables, we find that

$$b_{IJ} = \frac{k_{LCB I} K_J^- P_J}{(K_I^- + K_I^s + s)(k_{LCB1} P_1 + k_{LCB2} P_2 + s) + k_{LCB I} (K_1^- P_1 + K_2^- P_2)} \quad (19)$$

To calculate the bivariate distribution of degree of polymerization and number of branch points per molecule, we need to define three further parameters. The self-similarity of the polymer chains ensures that all the chain strands (i.e., chain sections between branch points or chain ends) formed at catalyst site  $I$  are distributed according to the same Flory distribution, with a mean degree of polymerization which we define as  $N_{xI}$ . We evaluate these distributions in Appendix A and demonstrate that (provided  $N_{xI} \gg 1$ )

$$N_{xI} = \frac{k_{pI} M (k_{LCB1} P_1 + k_{LCB2} P_2 + s)}{(K_I^- + K_I^s + s)(k_{LCB1} P_1 + k_{LCB2} P_2 + s) + k_{LCB I} (K_1^- P_1 + K_2^- P_2)} \quad (20)$$

Finally, since they obey two separate probability distributions, we need to know the fraction  $f_1$  of chains in the reactor that are catalyst 1 chains ( $P_1$ ,  $D_1^-$ , or  $D_1^s$ ) and the fraction  $f_2 = 1 - f_1$  that are catalyst 2 chains ( $P_2$ ,  $D_2^-$ , or  $D_2^s$ ). We find

$$\begin{aligned} f_1 &= \frac{P_1 + D_1^- + D_1^s}{P_1 + D_1^- + D_1^s + P_2 + D_2^- + D_2^s} \\ &= \frac{P_1 ((K_1^s + s)(k_{LCB1} P_1 + k_{LCB2} P_2 + s) + K_1^- s)}{(P_1 (K_1^s + s) + P_2 (K_2^s + s))(k_{LCB1} P_1 + k_{LCB2} P_2 + s) + s(K_1^- P_1 + K_2^- P_2)} \end{aligned} \quad (21)$$

Together, the six parameters  $b_{11}$ ,  $b_{12}$ ,  $b_{22}$ ,  $N_1$ ,  $N_2$ , and  $f_1$  are sufficient to characterize the full molecular weight and branching distribution of the two-catalyst system. One might, additionally, wish to obtain the relative populations of living chains, macromonomers and dead chains within each of the chain populations, which would require extra parameters, but these do not affect the overall molecular weight and branching distributions.

When considering the seniority and priority distributions, we find it convenient to define an auxiliary

parameter,  $r$ , which is the ratio of catalyst-1 chain strands to catalyst-2 chain strands.

$$r = \frac{S_1}{S_2} \quad (22)$$

In terms of the other variables, we find

$$r = \frac{b_{21}(1 - f_1) + (1 - 2b_{22} - b_{21})f_1}{(1 - 2b_{11} - b_{12})(1 - f_1) + b_{12}f_1} \quad (23)$$

**3.2. Branching and Molecular Weight Distributions When One Catalyst Is "Linear".** We consider first the case where catalyst 2 is a "linear" catalyst; i.e., it does not form branches by the polymerization of macromonomers ( $k_{LCB2} = 0$ ). This means that there are no  $B_{22}$  or  $B_{21}$  branch points, and  $b_{22} = b_{21} = 0$ . In this special case, we are able to derive explicit algebraic expressions for the branching and molecular weight distributions.

Following the methodology of ref 15, we first obtain the probability distribution  $p_{n,n_L}$  of the number  $n$  of branches of type  $B_{11}$  and number  $n_L$  of branches of type  $B_{12}$  that are present on "branching catalyst chains" ( $P_1$ ,  $D_1^-$ , or  $D_1^S$ ). Because of the self-similarity of the branched polymer chains, the same probability distribution applies to any sub-branches that begin with a chain strand formed on the branching catalyst. We can define a generating function

$$F(y, z) = \sum_{n, n_L=0}^{\infty} p_{n,n_L} y^n z^{n_L} \quad (24)$$

In the upstream direction, a catalyst 1 strand is followed by an initiation site with probability  $t_1 = 1 - b_{11} - b_{12}$ , a  $B_{11}$  branch point (and so two more catalyst 1 strands) with probability  $b_{11}$  or a  $B_{12}$  branch point (and so one linear catalyst 2 strand and one catalyst 1 strand) with probability  $b_{12}$ . Hence

$$F = t_1 + b_{11}yF^2 + b_{12}zF \quad (25)$$

This is a quadratic equation for the generating function  $F$ , which can be solved and expanded as a power series in  $y$  and  $z$  to give

$$p_{n,n_L} = \frac{(2n + n_L)!}{n!(n+1)!n_L!} b_{11}^n b_{12}^{n_L} t_1^{n+1} \quad (26)$$

A chain with  $n$  of branches of type  $B_{11}$  and number  $n_L$  of branches of type  $B_{12}$  contains  $2n + n_L + 1$  branching catalyst 1 chain strands (each distributed according to a Flory distribution with mean degree of polymerization  $N_{x1}$ ) and  $n_L$  linear catalyst 2 chain strands (each distributed according to a Flory distribution with mean degree of polymerization  $N_{x2}$ ). For  $s$  strands each with a Flory distribution of mean  $N_x$  the overall degree of polymerization obeys a distribution

$$P(N) = \frac{N^{s-1}}{N_x^s (s-1)!} \exp\left(-\frac{N}{N_x}\right) \quad (27)$$

We now define  $N_1$  to be the total degree of polymerization of the strands on the molecule that were polymer-

ized at catalyst 1, and  $N_2$  to be the total degree of polymerization of the strands on the molecule that were polymerized at catalyst 2. The total degree of polymerization is  $N = N_1 + N_2$ . At fixed numbers of branches,  $N_1$  and  $N_2$  each individually obey a distribution of the form in eq. 27. Hence, the probability distribution of  $N_1$ ,  $N_2$ ,  $n$ , and  $n_L$  for a branching catalyst chain is

$$P_B(N_1, N_2, n, n_L) = \frac{b_{11}^n b_{12}^{n_L} t_1^{n+1}}{n!(n+1)!n_L!(n_L-1)!N_{x1}N_{x2}} \times \left(\frac{N_1}{N_{x1}}\right)^{2n+n_L} \left(\frac{N_2}{N_{x2}}\right)^{n_L-1} \exp\left(-\frac{N_1}{N_{x1}} - \frac{N_2}{N_{x2}}\right), \quad n_L \neq 0 \quad (28)$$

The case  $n_L = 0$  has to be treated separately, because there are no catalyst 2 strands. This gives

$$P_B(N_1, N_2, n, n_L) = \frac{b_{11}^n t_1^{n+1}}{n!(n+1)!N_{x1}} \left(\frac{N_1}{N_{x1}}\right)^{2n} \exp\left(-\frac{N_1}{N_{x1}}\right) \delta(N_2), \quad n_L = 0 \quad (29)$$

From the probability distribution  $P_B(N_1, N_2, n, n_L)$ , one can obtain the probability distribution of degree of polymerization  $N = N_1 + N_2$  and number of branches  $\beta = n + n_L$  on a branching catalyst chain by summing and integrating over all combinations of  $N_1$ ,  $N_2$ ,  $n$ , and  $n_L$  that give these values.

$$P_B(N, \beta) = \frac{b_{11}^\beta t_1^{\beta+1}}{\beta!(\beta+1)!N_{x1}} \left(\frac{N}{N_{x1}}\right)^{2\beta} \exp\left(-\frac{N}{N_{x1}}\right) + \int_0^N dN_2 \sum_{n_L=1}^{\beta} P_B(N_1 = N - N_2, N_2, n = \beta - n_L, n_L) \quad (30)$$

The sum and integral in this equation must be evaluated numerically, but this poses no major problems.

The probability distribution for the degree of polymerization  $N$  on a branching catalyst chain is obtained by additionally summing over the total number of branches (i.e., all possible combinations of  $n$  and  $n_L$ ) and this gives

$$P_B(N) = \frac{t_1}{N\sqrt{b_{11}t_1}} I_1\left(2\frac{N}{N_{x1}}\sqrt{b_{11}t_1}\right) \exp\left(-\frac{N}{N_{x1}}\right) + \int_0^N dN_2 P_T(N_1 = N - N_2, N_2) \quad (31)$$

where

$$P_T(N_1, N_2) = \frac{b_{12}t_1}{\sqrt{N_1N_2N_{x1}N_{x2}b_{11}b_{12}t_1}} I_1\left(2\frac{N_1}{N_{x1}}\sqrt{b_{11}t_1}\right) \times I_1\left(2\sqrt{\frac{b_{12}N_1N_2}{N_{x1}N_{x2}}}\right) \exp\left(-\frac{N_1}{N_{x1}} - \frac{N_2}{N_{x2}}\right) \quad (32)$$

and  $I_1(x)$  is a modified Bessel function of the first kind and order 1. The linear catalyst chains contain no branches and have degrees of polymerization distributed according to the Flory distribution

$$P_L(N) = \frac{1}{N_{x2}} \exp\left(-\frac{N}{N_{x2}}\right) \quad (33)$$

Hence, the probability distribution of branching and

degree of polymerization for a chain chosen randomly from the reactor population is

$$P(N, \beta) = f_1 P_B(N, \beta) + f_2 P_L(N) \delta_\beta \quad (34)$$

and the probability distribution of degree of polymerization is

$$P(N) = f_1 P_B(N) + f_2 P_L(N) \quad (35)$$

Clearly, in the limit of no linear catalyst ( $f_2 = 0$ ,  $b_{12} = 0$ ) these expressions reduce to those derived previously<sup>11–16</sup> for the single branching metallocene system.

**3.3. Branching and Molecular Weight Distributions in the General Case.** We cannot presently obtain explicit algebraic expressions for the branching and molecular weight distribution when both catalysts admit branches. We can, however, obtain these implicitly, as we shall now describe. It is clear from the previous section that it is advantageous to obtain information about the number of chain strands on a given molecule that were formed by polymerization on each of the catalyst sites. Using this idea, we aim to obtain the probability  $q_{I,j,k}$  that a chain currently on catalyst  $I$  contains  $j$  strands formed at catalyst 1 and  $k$  strands formed at catalyst 2. Because of the self-similarity of the branched polymer chains, the same probability distributions apply to any sub-branches that begin with a chain strand formed on the relevant catalyst. We can define generating functions

$$F_1(y, z) = \sum_{j,k=0}^{\infty} q_{1,j,k} y^j z^k \quad (36)$$

$$F_2(y, z) = \sum_{j,k=0}^{\infty} q_{2,j,k} y^j z^k \quad (37)$$

In the upstream direction, a catalyst 1 strand is followed by an initiation site with probability  $t_1 = 1 - b_{11} - b_{12}$ , a B<sub>11</sub> branch point with probability  $b_{11}$  or a B<sub>12</sub> branch point with probability  $b_{12}$ . Hence

$$F_1 = y(t_1 + b_{11}F_1^2 + b_{12}F_1F_2) \quad (38)$$

and, similarly

$$F_2 = z(t_2 + b_{22}F_2^2 + b_{21}F_1F_2) \quad (39)$$

where  $t_2 = 1 - b_{22} - b_{21}$ . If one could solve eqs 38 and 39 and expand in powers of  $y$  and  $z$ , then one could obtain explicit algebraic expressions for  $q_{I,j,k}$ . However, the two equations reduce to a quartic in either  $F_1$  or  $F_2$  which makes such a procedure difficult. Similar problems are encountered when using the generating function formalism on systems with branch point functionalities greater than 3.

Instead, we substitute from (36) and (37) into (38) and (39) and equate terms with identical powers of  $y$  and  $z$ . This yields, for  $j + k > 1$

$$q_{1,j,k} = \sum_{j'=0}^{j-1} \sum_{k'=0}^k (b_{11} q_{1,j',k'} q_{1,j-j'-1,k-k'} + b_{12} q_{1,j',k'} q_{2,j-j'-1,k-k'}) \quad (40)$$

$$q_{2,j,k} = \sum_{j'=0}^j \sum_{k'=0}^{k-1} (b_{22} q_{2,j',k'} q_{2,j-j',k-k'-1} + b_{21} q_{2,j',k'} q_{1,j-j',k-k'-1}) \quad (41)$$

and

$$q_{1,1,0} = t_1$$

$$q_{1,0,1} = 0$$

$$q_{1,0,0} = 0$$

$$q_{2,1,0} = 0$$

$$q_{2,0,1} = t_2$$

$$q_{2,0,0} = 0$$

The recursion relations 40 and 41 can be used to generate the probability distributions  $q_{I,j,k}$ . This can be done numerically, and is very rapid for reasonable numbers of chain strands (it is rare to need these for more than, e.g., 60 chain strands in total). One can make use of the fact that

$$q_{1,0,k} = 0$$

$$q_{2,j,0} = 0$$

$$q_{I,j,k} = 0, \text{ for } j + k \text{ even}$$

though these are generated automatically by (40) and (41) and, in fact, the most time-consuming part of the generation of the MWD and branching distribution lies in the final summation and integration defined below.

These recursion relations are similar to those obtained by Costeux<sup>24</sup> for the branching distribution in the same chemical system. It is more advantageous to obtain the strand distribution, as is done here, because it allows one to obtain exact (rather than approximate) predictions of the molecular weight distribution.

Having obtained the probability distributions  $q_{I,j,k}$ , one can obtain the probability that a chain picked at random from the reaction bath has  $N_1$  monomers in  $j$  strands of type 1 and  $N_2$  monomers in  $k$  strands of type 2. This derivation proceeds in a manner analogous to that of the previous section. We sum over chains from both the catalysts, giving, for  $j \neq 0$  and  $k \neq 0$ ,

$$P(N_1, N_2, j, k) = (f_1 q_{1,j,k} + f_2 q_{2,j,k}) \frac{N_1^{j-1} N_2^{k-1}}{(j-1)!(k-1)! N_{x1}^j N_{x2}^k} \exp\left(-\frac{N_1}{N_{x1}} - \frac{N_2}{N_{x2}}\right) \quad (42)$$

and

$$P(N_1, N_2, j, 0) = f_1 q_{1,j,0} \frac{N_1^{j-1}}{(j-1)! N_{x1}^j} \exp\left(-\frac{N_1}{N_{x1}}\right) \delta(N_2) \quad (43)$$

$$P(N_1, N_2, 0, k) = f_2 q_{2,0,k} \frac{N_2^{k-1}}{(k-1)! N_{x2}^k} \exp\left(-\frac{N_2}{N_{x2}}\right) \delta(N_1) \quad (44)$$



To obtain the molecular weight and degree of branching distribution, note that a molecule with  $j + k$  strands contains  $\beta = (j + k - 1)/2$  branch points. Hence, one must sum over all combinations of  $j$  and  $k$  that give a branching number  $\beta$ , and integrate over all combinations of  $N_1$  and  $N_2$  that give a molecular weight  $N$ ;

$$P(N, \beta) = f_1 q_{1, 2\beta+1, 0} \frac{N^{2\beta}}{(2\beta)! N_{x1}^{2\beta+1}} \exp\left(-\frac{N}{N_{x1}}\right) + f_2 q_{2, 0, 2\beta+1} \frac{N^{2\beta}}{(2\beta)! N_{x2}^{2\beta+1}} \exp\left(-\frac{N}{N_{x2}}\right) + (1 - \delta_\beta) \int_0^N dN_2 \sum_{j=1}^{2\beta} P(N_1 = N - N_2, N_2, j, k = 2\beta + 1 - j) \quad (45)$$

Since we cannot obtain an explicit form for this, to obtain the probability distribution of the molecular weight alone one must numerically sum over the number of branches

$$P(N) = \sum_{\beta} P(N, \beta)$$

where the sum is terminated at an appropriately high value of  $\beta$  to obtain sufficient accuracy.

**3.4. Averages over the Molecular Weight and Branching Distribution.** The generating functions  $F_1$  and  $F_2$  obtained in the previous section can be used to derive certain averages over the distribution. For example, the mean number of chain strands of type 1 on a catalyst 1 chain is

$$\bar{j}_1 = \sum_{j,k=0}^{\infty} j q_{1,j,k} = \left. \frac{\partial F_1}{\partial y} \right|_{y=z=1} \quad (46)$$

One can obtain this by differentiating eqs 38 and 39 with respect to  $y$  and setting  $y = z = 1$  (note that  $F_1 = F_2 = 1$  in this limit). This gives two simultaneous equations in  $\partial F_1 / \partial y|_{y=z=1}$  and  $\partial F_2 / \partial y|_{y=z=1}$  which can be solved to give the mean number of chain strands of type 1 on catalyst 1 and catalyst 2 chains

$$\bar{j}_1 = \left. \frac{\partial F_1}{\partial y} \right|_{y=z=1} = \frac{1 - 2b_{22} - b_{21}}{(1 - 2b_{11} - b_{12})(1 - 2b_{22} - b_{21}) - b_{12}b_{21}} \quad (47)$$

$$\bar{j}_2 = \left. \frac{\partial F_2}{\partial y} \right|_{y=z=1} = \frac{b_{21}}{(1 - 2b_{11} - b_{12})(1 - 2b_{22} - b_{21}) - b_{12}b_{21}} \quad (48)$$

Similarly, one can obtain the mean number of chain strands of type 2 on catalyst 1 and catalyst 2 chains as

$$\bar{k}_1 = \left. \frac{\partial F_1}{\partial z} \right|_{y=z=1} = \frac{b_{12}}{(1 - 2b_{11} - b_{12})(1 - 2b_{22} - b_{21}) - b_{12}b_{21}} \quad (49)$$

$$\bar{k}_2 = \left. \frac{\partial F_2}{\partial z} \right|_{y=z=1} = \frac{1 - 2b_{11} - b_{12}}{(1 - 2b_{11} - b_{12})(1 - 2b_{22} - b_{21}) - b_{12}b_{21}} \quad (50)$$

The number-average degree of polymerization over the whole distribution is then

$$N_n = f_1(N_{x1}\bar{j}_1 + N_{x2}\bar{k}_1) + f_2(N_{x1}\bar{j}_2 + N_{x2}\bar{k}_2) \quad (51)$$

The mean number of branches per molecule is

$$\beta_n = \frac{f_1(\bar{j}_1 + \bar{k}_1) + f_2(\bar{j}_2 + \bar{k}_2) - 1}{2} \quad (52)$$

and the ratio of the number of long chain branches per 1000C is

$$\lambda = 500 \frac{\beta_n}{N_n} \quad (53)$$

**3.5. Seniority and Priority Distributions.** In ref 15, two rheologically relevant topological variables were defined for each chain strand in a branched polymer: seniority and priority. The *seniority* of a given polymer strand may be evaluated by counting the number of strands to the furthest free end in each chain direction (inclusive of the current strand, so the minimum seniority is 1). The strand seniority is then the smaller of the two values. The seniority is considered to be relevant to the rheological relaxation time of that strand. The *priority* of a given strand may be calculated by counting the number of free ends attached in each chain direction and then taking the smaller value from the two directions. The priority is related to the maximum stretch that a chain strand can achieve within the entanglement "tube" and is an important parameter when considering the limits of extension hardening of the melt.

For a detailed discussion of how these parameters might be related to rheological models for the melt, we refer the reader to ref 15. Here we shall limit ourselves to an evaluation of the statistical distribution of these two quantities over the dual-catalyst ensemble. Since the seniority statistic is strictly applicable only when chain stands are of equal length, we shall consider only the case where that average strand lengths are equal ( $N_1 = N_2$ ). Even here, as noted in ref 15, one is relying on a degree of averaging over the actual lengths of successive strands, which individually obey the Flory distribution as discussed above.

Since seniority and priority each require examination of the chain structure in both directions from a given chain strand, we need to consider *downstream* as well as upstream branching probabilities. We use the notation that the probability of a branch point of type  $B_{IJ}$  being immediately downstream from a strand of type  $K$  is  $b_{IJ,K}^D$ . We consider first the catalyst 1 strands.



Because there are two such strands upstream from a B<sub>11</sub> branch point, the probability of a B<sub>11</sub> branch point being downstream from a catalyst 1 strand is

$$b_{11,1}^D = \frac{2B_{11}}{S_1} = 2b_{11} \quad (54)$$

There is only one catalyst-1 stand upstream from either a B<sub>12</sub> or B<sub>21</sub> branch point, and so

$$b_{12,1}^D = \frac{B_{12}}{S_1} = b_{12} \quad (55)$$

$$b_{21,1}^D = \frac{B_{21}}{S_1} = \frac{b_{21}}{r} \quad (56)$$

where  $r = S_1/S_2$  as defined above. The probability of hitting a chain end downstream from a catalyst 1 strand is

$$t_1^D = 1 - b_{11,1}^D - b_{12,1}^D - b_{21,1}^D \quad (57)$$

Similarly

$$b_{22,2}^D = \frac{2B_{22}}{S_2} = 2b_{22} \quad (58)$$

$$b_{21,2}^D = \frac{B_{21}}{S_2} = b_{21} \quad (59)$$

$$b_{12,2}^D = \frac{B_{12}}{S_2} = rb_{12} \quad (60)$$

$$t_2^D = 1 - b_{22,2}^D - b_{21,2}^D - b_{12,2}^D \quad (61)$$

We now generalize the methods developed in ref 15 to the dual catalyst system. Throughout the following, we use superscripts 1U to denote a statistic for a catalyst 1 strand in the upstream direction and 1D for a catalyst 1 strand in the downstream direction (similarly 2U and 2D for catalyst 2 strands).

**3.5.1. Seniority Distribution.** This is most straightforwardly obtained using the cumulative seniority distribution. We consider the seniority in the upstream and downstream directions separately, and define

$f_m^{1U} = P$  (upstream seniority from catalyst 1 strand  $\leq m$ )

and similarly define  $f_m^{1D}$ ,  $f_m^{2U}$ , and  $f_m^{2D}$ . If a strand is branched in a given direction, then it has seniority  $\leq m$  only if the subsequent two strands have seniority  $\leq m - 1$ . Hence, noting that an upstream branch is followed by two upstream strands, but a downstream branch is followed by one upstream and one downstream strand, we find

$$f_m^{1U} = t_1 + b_{11}[f_{m-1}^{1U}]^2 + b_{12}f_{m-1}^{1U}f_{m-1}^{2U} \quad (62)$$

$$f_m^{2U} = t_2 + b_{22}[f_{m-1}^{2U}]^2 + b_{21}f_{m-1}^{1U}f_{m-1}^{2U} \quad (63)$$

$$f_m^{1D} = t_1^D + 2b_{11}f_{m-1}^{1U}f_{m-1}^{1D} + b_{12}f_{m-1}^{1D}f_{m-1}^{2U} + \frac{b_{21}}{r}f_{m-1}^{2D}f_{m-1}^{2U} \quad (64)$$

$$f_m^{2D} = t_2^D + 2b_{22}f_{m-1}^{2U}f_{m-1}^{2D} + b_{21}f_{m-1}^{2D}f_{m-1}^{1U} + rb_{12}f_{m-1}^{1D}f_{m-1}^{1U} \quad (65)$$

These recursion relations allow  $f_m^{1U}$ ,  $f_m^{1D}$ ,  $f_m^{2U}$ , and  $f_m^{2D}$  to be evaluated for all  $m$  given

$$f_1^{1U} = t_1$$

$$f_1^{2U} = t_2$$

$$f_1^{1D} = t_1^D$$

$$f_1^{2D} = t_2^D$$

$t_2^D$  The probability  $s_m^{1U}$  of obtaining upstream seniority  $m$  on a catalyst 1 strand is thus

$$s_m^{1U} = f_m^{1U} - f_{m-1}^{1U} \quad (66)$$

Since the seniority of a given strand is the smaller of the upstream and downstream seniorities, the probability  $s_m^1$  of obtaining seniority  $m$  on a catalyst 1 strand is thus

$$s_m^1 = s_m^{1U}(1 - f_m^{1D}) + s_m^{1D}(1 - f_m^{1U}) + s_m^{1U}s_m^{1D} \quad (67)$$

and similarly for catalyst 2 strands. The seniority distribution averaged over all the strands in the system is

$$s_m = \frac{rs_m^1 + s_m^2}{r + 1} \quad (68)$$

**3.5.2. Priority distribution.** This is most easily evaluated using a similar generating function formalism to that used above in the calculation of the branching distribution. We define a probability  $p_k^{1U}$  of obtaining upstream priority  $k$  for a catalyst 1 strand, and an associated generating function

$$F^{1U} = \sum_{k=1}^{\infty} p_k^{1U} z^k \quad (69)$$

(and similarly for 1D, 2U, and 2D). Since the priority of a given strand is the sum of the priorities of the two subsequent strands following a branch point, we find

$$F^{1U} = t_1 z + b_{11}[F^{1U}]^2 + b_{12}F^{1U}F^{2U} \quad (70)$$

$$F^{2U} = t_2 z + b_{22}[F^{2U}]^2 + b_{21}F^{1U}F^{2U} \quad (71)$$

$$F^{1D} = t_1^D z + 2b_{11}F^{1U}F^{1D} + b_{12}F^{1D}F^{2U} + \frac{b_{21}}{r}F^{2D}F^{2U} \quad (72)$$

$$F^{2D} = t_2^D z + 2b_{22}F^{2U}F^{2D} + b_{21}F^{2D}F^{1U} + rb_{12}F^{1D}F^{1U} \quad (73)$$

In the case where one catalyst is linear, it is possible to obtain explicit analytical formulas for the priority distribution, but this is no faster to evaluate numerically than the implicit scheme we now develop. We substitute the series expansions of form 69 into the above formulas, and equate terms with equal powers of  $z$  to give

$$p_k^{1U} = \sum_{k'=1}^{k-1} b_{11} p_k^{1U} p_{k-k'}^{1U} + b_{12} p_k^{1U} p_{k-k'}^{2U} \quad (74)$$

$$p_k^{2U} = \sum_{k'=1}^{k-1} b_{22} p_k^{2U} p_{k-k'}^{2U} + b_{21} p_k^{1U} p_{k-k'}^{2U} \quad (75)$$

$$p_k^{1D} = \sum_{k'=1}^{k-1} 2b_{11} p_k^{1U} p_{k-k'}^{1D} + b_{12} p_k^{1D} p_{k-k'}^{2U} + \frac{b_{21}}{r} p_k^{2D} p_{k-k'}^{2U} \quad (76)$$

$$p_k^{2D} = \sum_{k'=1}^{k-1} 2b_{22} p_k^{2U} p_{k-k'}^{2D} + b_{21} p_k^{2D} p_{k-k'}^{1U} + r b_{12} p_k^{1D} p_{k-k'}^{1U} \quad (77)$$

together with the results for priority 1

$$p_1^{1U} = t_1$$

$$p_1^{2U} = t_2$$

$$p_1^{1D} = t_1^D$$

$$p_1^{2D} = t_2^D$$

These formulas can be applied recursively to generate the whole upstream and downstream priority distributions for each strand type. Since the priority of a given strand is the smaller of the upstream and downstream priorities, the probability of obtaining priority  $k$  on a catalyst 1 strand is

$$p_k^1 = p_k^{1U} [1 - \sum_{k'=1}^{k-1} p_k^{1D}] + p_k^{1D} [1 - \sum_{k'=1}^{k-1} p_k^{1U}] - p_k^{1U} p_k^{1D} \quad (78)$$

and similarly for catalyst 2. The priority distribution averaged over all strands in the ensemble is

$$p_k = \frac{r p_k^1 + p_k^2}{r + 1} \quad (79)$$

**3.5.3. Bivariate Distribution of Seniority and Priority.** For a catalyst 1 strand, we define a probability

$$g_{k,m}^{1U} = P(\text{upstream seniority} \leq m$$

$$\text{and upstream priority} = k)$$

together with an associated generating function

$$F_m^{1U} = \sum_{k=1}^{\infty} g_{k,m}^{1U} z^k \quad (80)$$

(and similarly for 1D, 2U, and 2D). The bivariate distribution of seniority and priority can be obtained from the relations

$$F_m^{1U} = t_1 z + b_{11} [F_{m-1}^{1U}]^2 + b_{12} F_{m-1}^{1U} F_{m-1}^{2U} \quad (81)$$

$$F_m^{2U} = t_2 z + b_{22} [F_{m-1}^{2U}]^2 + b_{21} F_{m-1}^{1U} F_{m-1}^{2U} \quad (82)$$

$$F_m^{1D} = t_1^D z + 2b_{11} F_{m-1}^{1U} F_{m-1}^{1D} + b_{12} F_{m-1}^{1D} F_{m-1}^{2U} + \frac{b_{21}}{r} F_{m-1}^{2D} F_{m-1}^{2U} \quad (83)$$

$$F_m^{2D} = t_2^D z + 2b_{22} F_{m-1}^{2U} F_{m-1}^{2D} + b_{21} F_{m-1}^{2D} F_{m-1}^{1U} + r b_{12} F_{m-1}^{1D} F_{m-1}^{1U} \quad (84)$$

Note that this gives the seniority generating formulas when  $z = 1$ , and the priority generating formulas in the limit  $m \rightarrow \infty$ . We substitute the series expansions of form 80 into the above formulas and equate terms with equal powers of  $z$  to give

$$g_{k,m}^{1U} = \sum_{k'=1}^{k-1} b_{11} g_{k',m-1}^{1U} g_{k-k',m-1}^{1U} + b_{12} g_{k',m-1}^{1U} g_{k-k',m-1}^{2U} \quad (85)$$

$$g_{k,m}^{2U} = \sum_{k'=1}^{k-1} b_{22} g_{k',m-1}^{2U} g_{k-k',m-1}^{2U} + b_{21} g_{k',m-1}^{1U} g_{k-k',m-1}^{2U} \quad (86)$$

$$g_{k,m}^{1D} = \sum_{k'=1}^{k-1} 2b_{11} g_{k',m-1}^{1U} g_{k-k',m-1}^{1D} + b_{12} g_{k',m-1}^{1D} g_{k-k',m-1}^{2U} + \frac{b_{21}}{r} g_{k',m-1}^{2D} g_{k-k',m-1}^{2U} \quad (87)$$

$$g_{k,m-1}^{2D} = \sum_{k'=1}^{k-1} 2b_{22} g_{k',m-1}^{2U} g_{k-k',m-1}^{2D} + b_{21} g_{k',m-1}^{2D} g_{k-k',m-1}^{1U} + r b_{12} g_{k',m-1}^{1D} g_{k-k',m-1}^{1U} \quad (88)$$

together with

$$g_{1,m}^{1U} = t_1$$

$$g_{1,m}^{2U} = t_2$$

$$g_{1,m}^{1D} = t_1^D$$

$$g_{1,m}^{2D} = t_2^D$$

$$g_{k,1}^{1U} = g_{k,1}^{2U} = g_{k,1}^{1D} = g_{k,1}^{2D} = 0, \quad k > 1$$

These recursion relations can be used to obtain  $g_{k,m}^{1U}$  and hence the probability of a catalyst 1 strand having upstream seniority  $m$  and upstream priority  $k$  as

$$w_{k,m}^{1U} = g_{k,m}^{1U} - g_{k,m-1}^{1U} \quad (89)$$

and similarly for 1D, 2U, and 2D. The overall distribution for both directions for catalyst 1 strands is

$$w_{k,m}^1 = w_{k,m}^{1U} \sum_{\substack{k' \geq k \\ m' \geq m}} w_{k',m'}^{1D} + \sum_{m' > m} w_{k,m'}^{1U} \sum_{k' \geq k} w_{k',m'}^{1D} + \sum_{k' > k} w_{k',m}^{1U} \sum_{m' \geq m} w_{k',m'}^{1D} + w_{k,m}^{1U} \sum_{\substack{k' > k \\ m' > m}} w_{k',m'}^{1D} \quad (90)$$

and similarly for catalyst 2 strands. The average

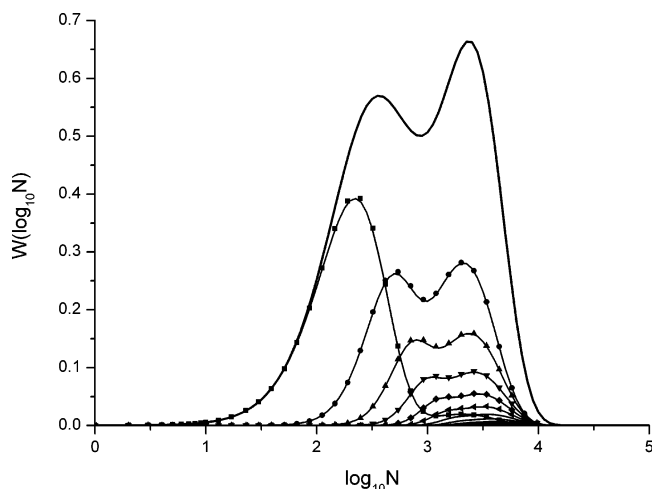


**Figure 2.** Overall molecular weight distribution (thick line) and weight distributions at fixed branch number for chains from 0 to 10 branches (thin lines) for the parameters  $b_{11} = 0.1513$ ,  $b_{12} = 0.06051$ ,  $b_{22} = 0$ ,  $N_1 = 110.3$ ,  $N_2 = 1048.3$ , and  $f_1 = 0.995893$ . Also shown are results (symbols), from the population balance approach, using parameters  $P_1 = 1 \times 10^{-3}$ ,  $P_2 = 4 \times 10^{-4}$ ,  $M = 7$ ,  $k_{p1} = 100$ ,  $k_{p2} = 150$ ,  $k_{LCB1} = 40$ ,  $k_{LCB2} = 0$ ,  $K_1^- = 1$ ,  $K_2^- = 1$ ,  $K_1^s = 4$ ,  $K_2^s = 0$ , and  $s = 600^{-1}$  in arbitrary units. Symbols are squares (no branches), circles (one branch), up triangles (two branches), down triangles (three branches), diamonds (four branches), left triangles (five branches).

distribution over all strands is obtained from

$$w_{k,m} = \frac{r w_{k,m}^1 + w_{k,m}^2}{r + 1} \quad (91)$$

#### 4. Results

**4.1. Branching and Molecular Weight Distribution.** To verify the above results for branching and molecular weight distributions, in this section we compare these calculations with direct solution of the population balance equations for this system. The latter are detailed in Appendix B, and reflect the more conventional (but numerically much lengthier) approach to solution of the branching and molecular weight distribution for metallocene systems.<sup>12,25,26</sup> We show, in Figures 2–4, some sample molecular weight and branching distributions for various combinations of the parameters  $b_{11}$ ,  $b_{12}$ ,  $b_{22}$ ,  $N_1$ ,  $N_2$ , and  $f_1$  (values shown in figure captions). Results are shown for weight fraction distributions, normalized on a  $\log N$  axis;

$$W(\log_{10} N, \beta) = \ln 10 \frac{N^\beta P(N, \beta)}{N_n} \quad (92)$$

Figures 2 and 3 represent the case where one catalyst is linear ( $b_{22} = b_{21} = 0$ ). Figure 4 is for the more general case where both catalysts branch. Although the bivariate distribution is shown only up to 10 branches in Figure 4, to obtain convergence of the overall molecular weight distribution (particularly the high molecular weight tail) required a summation over structures with up to 50 branches. Even so, the numerical calculation took less than a minute to perform on a PC. Such a summation is not necessary in Figures 2 and 3 because we have an explicit form for the overall MWD.

Also shown are the results for up to five branches obtained from the population balance approach, together with the kinetic parameters used to obtain these. It can

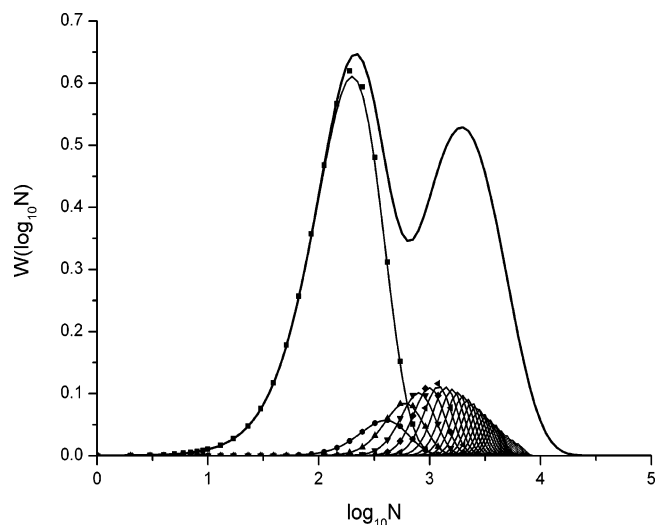


**Figure 3.** Overall molecular weight distribution (thick line) and weight distributions at fixed branch number for chains from 0 to 30 branches (thin lines) for the parameters  $b_{11} = 0.05564$ ,  $b_{12} = 0.6954$ ,  $b_{22} = 0$ ,  $N_1 = 100.0$ ,  $N_2 = 100.0$ , and  $f_1 = 0.11189$ . Also shown are results (symbols as for Figure 2), from the population balance approach, using parameters  $P_1 = 4 \times 10^{-4}$ ,  $P_2 = 1 \times 10^{-3}$ ,  $M = 2$ ,  $k_{p1} = 101.1$ ,  $k_{p2} = 90.17$ ,  $k_{LCB1} = 5$ ,  $k_{LCB2} = 0$ ,  $K_1^- = 0.3$ ,  $K_2^- = 1.5$ ,  $K_1^s = 0.2$ ,  $K_2^s = 0.3$ , and  $s = 300^{-1}$  in arbitrary units.

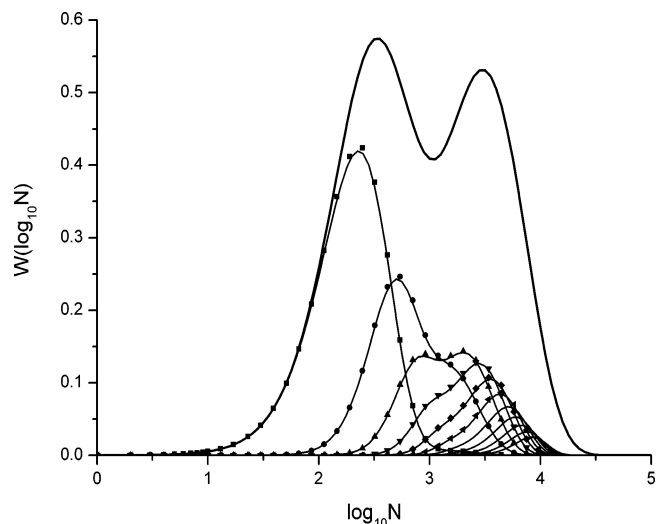


**Figure 4.** Overall molecular weight distribution (thick line) and weight distributions at fixed branch number for chains from 0 to 10 branches (thin lines) for the parameters  $b_{11} = 0.1314$ ,  $b_{12} = 0.05256$ ,  $b_{22} = 0.10289$ ,  $N_1 = 114.2$ ,  $N_2 = 670.7$ , and  $f_1 = 0.996521$ . Also shown are results (symbols as for Figure 2), from the population balance approach, using parameters  $P_1 = 1 \times 10^{-3}$ ,  $P_2 = 4 \times 10^{-4}$ ,  $M = 7$ ,  $k_{p1} = 100$ ,  $k_{p2} = 150$ ,  $k_{LCB1} = 40$ ,  $k_{LCB2} = 20$ ,  $K_1^- = 1$ ,  $K_2^- = 1$ ,  $K_1^s = 4$ ,  $K_2^s = 0$ , and  $s = 600^{-1}$  in arbitrary units.

be seen that the agreement between the two approaches is very good, but not perfect. The difference is due to the slightly different treatment of chain initiation between the two approaches and the allowed chemical behavior of the initiating species (as discussed in Appendix B). The parameters were chosen so as to indicate this difference, which is of order 1–2% for this set of parameters. In fact, the error is on the order of the inverse of the typical strand degree of polymerization in the system. Figure 6 uses exactly the same parameters as Figure 2, but the typical chain lengths are decreased or increased by a factor of 3. The discrepancy

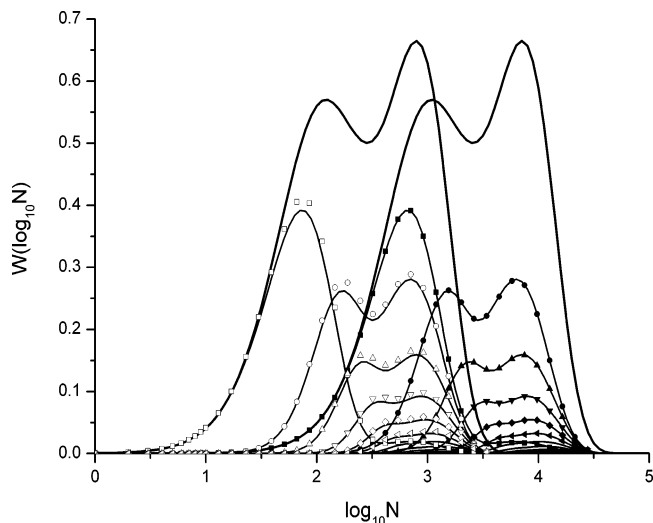


**Figure 5.** Overall molecular weight distribution (thick line) and weight distributions at fixed branch number for chains from 0 to 10 branches (thin lines) for identical parameters to Figure 2 except  $N_{x1} = 36.8$ ,  $N_{x2} = 349.4$  (left-hand curves) or  $N_{x1} = 330.9$ ,  $N_{x2} = 3144.9$  (right-hand curves). Also shown are results from the population balance approach, using identical parameters to Figure 2 but with  $k_{p1} = 33.333$ ,  $k_{p2} = 50$  (open symbols) or  $k_{p1} = 300$ ,  $k_{p2} = 450$  (filled symbols).

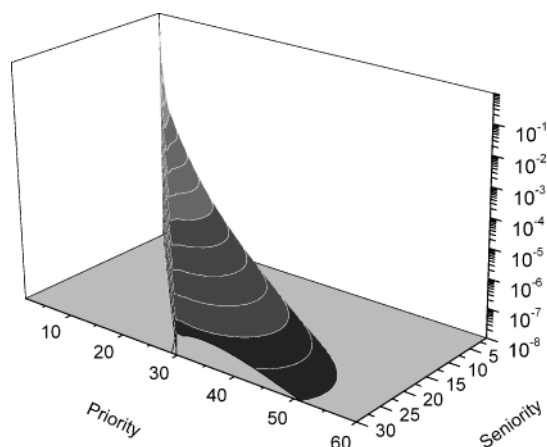


**Figure 6.** Bivariate seniority and priority distribution for a melt with parameters as given for Figure 3.

ancy between the two approaches is increased or reduced by the same factor, respectively. For the shorter chain lengths the discrepancy is now very obvious, but for the longer chains it is now barely visible on the graph.

Figures 2 and 3 each show a “bimodal” molecular weight distribution. Clearly, such a distribution is obtained when the polymerization at one of the catalysts produces chains that are typically much longer than those from the other catalyst. This occurs when polymerization at one of the catalysts is much faster (giving longer polymers), or when chain transfer reactions occur more readily on the other catalyst (giving shorter polymers). If the catalysts are not asymmetric in this way, it is harder to obtain bimodal distributions. Although Figures 2 and 3 both fulfill these broad criteria, producing similar overall molecular weight distributions, they are quite different in their underlying structure, as is clear from the molecular weight distributions as a function of branching number. The parameters for Figure 2 give long chains at the linear catalyst and shorter chains at the branching catalyst. The high

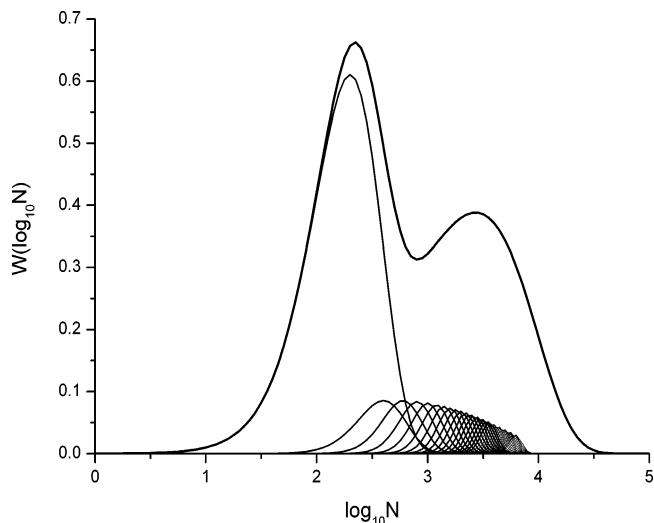


**Figure 7.** Overall molecular weight distribution (thick line) and weight distributions at fixed branch number for chains from 0 to 30 branches (thin lines) for the parameters  $b_{11} = 0.3534$ ,  $b_{12} = 0.1$ ,  $b_{22} = 0$ ,  $N_1 = 100.0$ ,  $N_2 = 100.0$ , and  $f_1 = 0.1854$ .

molecular weight portion of this distribution comprises both these long linear chains and branched chains in which long macromonomers from the linear catalyst have been incorporated into branched chains at the branching catalyst site. In contrast, the parameters for Figure 3 give short chains at the linear catalyst, but the parameters are such that there are many more macromonomers arising from this linear catalyst than from the branching catalyst. Hence, the branching catalyst produces quite long chains which incorporate a relatively large number of linear macromonomers. For this reason, the high molecular weight tail of this distribution is dominated by comblike polymers. The bimodal distribution of Figure 4 is obtained via a similar scheme to that of Figure 2, but now both polymers admit branches, and the overall distribution contains more branches.

**4.2. Seniority and Priority Distributions.** The parameters for Figure 3 were explicitly chosen so that the average strand lengths of catalyst 1 and catalyst 2 strands were equal ( $N_{x1} = N_{x2}$ ). In this case it is justified to calculate both the seniority and priority distribution. For this melt, the bivariate distribution of seniority and priority is shown in Figure 6. This distribution confirms the suggestion above that this melt is dominated by comblike polymers. For a pure melt of combs, the priority and seniority of each chain strand are equal. The distribution in Figure 6 is very strongly biased toward this limit (it is impossible to have a priority less than the seniority).

To illustrate how the topology of the melt can be varied in a multiple catalyst system, we show in Figure 7 the molecular weight distribution of another melt in which the second catalyst is linear ( $b_{22} = b_{21} = 0$ ). The parameters for this melt are chosen so that it has the same strand molecular weights and average number of branches per molecule,  $\beta_n$  as the melt of Figure 3. It also contains the same fraction of linear (unbranched) chain strands,  $r_{lin}$  which is given by

$$r_{lin} = \frac{rt_1^D + t_2^D}{r + 1} \quad (93)$$



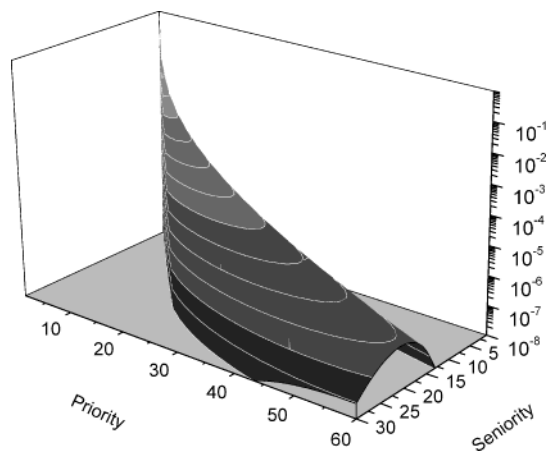


**Figure 8.** Bivariate seniority and priority distribution for a melt with parameters as given for Figure 7.

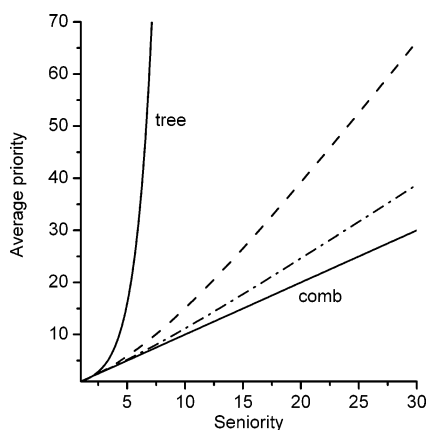


**Figure 9.** Average priority at fixed seniority for the melts with parameters as given in Figure 3 (dot-dash line) and Figure 7 (dash line). These are compared against the results for pure combs ( $k = m$ ) and pure Cayley trees ( $k = 2^{m-1}$ ).

These five constraints leave only one free parameter to vary. We choose this so that this melt has a higher probability that the branching catalyst incorporates branched macromonomers from the same catalyst (i.e.,  $b_{11}$  is significantly higher for Figure 7 than for Figure 3). The result on the distribution of seniority and priority, shown in Figure 8 is quite striking; as compared to Figure 6 this melt has a significantly higher typical priority for a given seniority. This is a direct result of the fact that the melt of Figure 7 has many more “branches-on-branches” than that of Figure 3. These differences between the two melts are illustrated further in Figure 9 which shows the average priority at fixed seniority for each melt, as compared against the “limiting” cases of a melt of pure combs and a melt of pure Cayley trees. It is virtually impossible to approach the Cayley tree limit in a statistical branching ensemble, but it appears quite possible to vary the proximity to the comb limit. Since priorities are related to the limit of extension hardening of a polymer melt, we would anticipate that larger priorities of the melt of Figure 7 would give rise to a greater degree of extension hardening as compared to the melt of Figure 3.

## 5. Conclusions

This paper serves to illustrate that the metallocene long chain branching mechanism does give “self-similar” chains in a CSTR, even with multiple metallocene catalysts, and that this self-similarity can be used to

derive useful information about the chain statistics. In this paper, we have focused on the branching and molecular weight distribution, and also the distribution of the rheologically relevant variables, “seniority” and “priority”. This approach has significant advantages over both the Monte Carlo<sup>23–25</sup> and population balance<sup>26</sup> methods as applied to these systems. Both the explicit analytical expressions and the implicit recursion schemes developed here are numerically *much* less intensive to evaluate than either rival approach. A further advantage of this approach over the population balance method is that it provides statistical information on the molecular architectures produced (without this, it would be impossible to derive, for example, the seniority and priority distributions).

As regards the development of *explicit* expressions for branching and molecular weight distribution, the generating function formalism used here appears to reach its limit at the case of a dual catalyst system with one catalyst linear (it is likely to be possible, if a little tedious, also to treat multiple linear catalysts with a single branching catalyst). Nevertheless, there is in principle no barrier to obtaining recursion formulas similar to those obtained here for multiple branching catalyst systems, should one wish to do so. We can foresee no problems with this in obtaining seniority, priority, or branching distributions. For the molecular weight distribution, as one increases the number of catalysts one also has to increase the dimensionality of the integral used to project the total degree of polymerization from the degrees of polymerization on each type of catalyst strand (in this paper we needed only to consider degrees of polymerization  $N_1$  and  $N_2$  on each type of catalyst strand, giving a one-dimensional integral to project onto  $N$ ). As the dimensionality of the integral increases, so the numerical cost of this method also increases; it might be that, for large numbers of catalysts, the population balance approach becomes a competitive method.

This paper has considered only the chain statistics arising from reaction in an ideal CSTR, in which an argument can be made for the self-similarity of the polymer chains. For batch and semibatch reactors (which are more common on a laboratory scale) no such argument can be made, and the chain statistics obtained here cannot be applied. In such cases, the only method presently available for the calculation of molecular weight and (approximate) branching distributions is the population balance approach.<sup>26</sup> It should be stressed, however, that population balance in itself gives no explicit information on the chain architecture, and cannot presently be used (for example) to obtain seniority and priority distributions, or other topological information. Nevertheless, in both batch and semibatch reactors, the *qualitative* description of the chain structure presented here in section 2.1 is still applicable and we would anticipate that this could prove useful in extending this work to the more challenging problem of obtaining chain statistics for these reactor types.

**Acknowledgment.** D.J.R. gratefully acknowledges the financial support of an EPSRC Advanced Research Fellowship.

## Appendix A. Strand Degrees of Polymerization

For chains strands formed on either catalyst, we need the probability distribution of the degree of polymeri-

zation  $N$ , which can be found from a detailed balance argument. Suppose  $[N]_I$  is the concentration of strands formed on catalyst  $I$  with degree of polymerization  $N$ . Then the kinetic equation for  $[N]_I$  is, for  $N > 0$

$$\frac{d[N]_I}{dt} = k_{pI}M[N-1]_I - k_{pI}M[N]_I - K_I^s[N]_I - K_I^{\overline{}}[N]_I - k_{LCBI}(D_1^{\overline{}} + D_2^{\overline{}})[N]_I - s[N]_I \quad (94)$$

from which, in steady-state conditions, we obtain

$$[N]_I = A_I[N-1]_I \quad (95)$$

where

$$A_I = \frac{k_{pI}M}{k_{pI}M + K_I^s + K_I^{\overline{}} + k_{LCBI}(D_1^{\overline{}} + D_2^{\overline{}}) + s} \quad (96)$$

The normalized probability distribution for the  $N$  is the Flory distribution:

$$P(N) = A_I^N(1 - A_I) \quad (97)$$

which has mean degree of polymerization

$$\begin{aligned} N_{xI} &= \frac{A_I}{1 - A_I} \\ &= \frac{k_{pI}M}{K_I^s + K_I^{\overline{}} + k_{LCBI}(D_1^{\overline{}} + D_2^{\overline{}}) + s} \end{aligned} \quad (98)$$

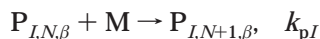
from which we obtain eq 20.

Note that, in deriving this result, we have used Flory distributions appropriate for the range  $0 \leq N \leq \infty$  (which is correct for chain strands beginning at a branch site) rather than  $1 \leq N \leq \infty$  (which is correct for chain strands beginning at an initiation site). Although there is a slight difference between these two cases, provided the stands are long ( $N_I \gg 1$ , which is the case if the polymerization rates are much larger than other rates in the reactor), it makes only a fractional difference to the overall molecular weight distribution but contributes to the small discrepancy with the population balance approach discussed in the main body of the paper. For most of the paper, we have used a continuum representation of the Flory distribution rather than the discrete one above.

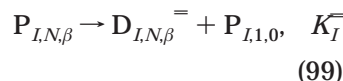
## Appendix B. Full Population Balance Equations

The full set of equations used in the populations balance scheme represent a generalization of the reaction mechanism used by Soares and Hamielec<sup>12</sup> and are as follows. The following reactions are included:

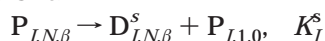
### 1. Monomer Addition



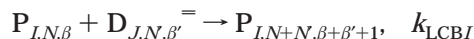
### 2. Chain Transfer to Double Bond



### 3. Chain Transfer to Dead Chain

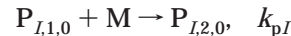


### 4. Long-Chain Branch Formation



where the subscripts  $I$ ,  $N$ , and  $\beta$  refer to catalyst type  $I$  ( $=1,2$ ), degree of polymerization  $N$ , and number of branches  $\beta$ . Comparing with the reaction mechanism used in the main body of this paper, it is clear that the empty catalyst site (C) is replaced in the present mechanism by the  $P_{I,1,0}$  species. This  $P_{I,1,0}$  species is allowed two separate reactions:

### 1. Monomer Addition



### 2. Long-Chain Branch Formation



so that its behavior is modeled in a slightly different fashion to the empty catalyst site (C) in the main body of the paper. This results in the population balance equations predicting very slightly different distributions to those obtained in this paper, but (as discussed in section 4) the differences between the two models disappear for large average degrees of polymerization of the strands between cross-links.

Following the method used by Soares and Hamielec,<sup>12</sup> one can write down rate equations for each of the species in the reactor and set the time derivatives to zero for steady state in a CSTR. This yields the following set of equations. For the double bond and dead chains,

$$D_{I,N,\beta}^{\overline{}} = \frac{K_I^{\overline{}}}{k_{LCB1}P_1 + k_{LCB2}P_2 + s} P_{I,N,\beta} \quad (101)$$

$$D_{I,N,\beta}^s = \frac{K_I^s}{s} P_{I,N,\beta} \quad (102)$$

where

$$P_I = \sum_{N=1}^{\infty} \sum_{\beta=0}^{\infty} P_{I,N,\beta} \quad (103)$$

For the living chains

$$\begin{aligned} P_{I,N,\beta} &= \frac{k_{pI}M}{\gamma_I} P_{I,N-1,\beta} + \\ &\quad \frac{k_{LCBI}^{N-1} \beta - 1}{\gamma_I} \sum_{N=1}^{\infty} \sum_{\beta'=0}^{\infty} P_{I,N-N,\beta'} (D_{1,N,\beta-\beta'-1}^{\overline{}} + D_{2,N,\beta-\beta'-1}^{\overline{}}) \end{aligned} \quad (104)$$

where

$$\gamma_I = k_{pI}M + K_I^s + K_I^{\overline{}} + k_{LCBI}(D_1^{\overline{}} + D_2^{\overline{}}) + s \quad (105)$$

$$D_I^{\overline{}} = \sum_{N=1}^{\infty} \sum_{\beta=0}^{\infty} D_{I,N,\beta}^{\overline{}} = \frac{K_I^{\overline{}}}{k_{LCB1}P_1 + k_{LCB2}P_2 + s} P_I \quad (106)$$

Combining (101) and (104) gives

$$P_{I,N,\beta} = A_I P_{I,N-1,\beta} + \sum_{N=1}^{N-1} \sum_{\beta'=0}^{\beta-1} \sum_{J=1}^2 L_{IJ} P_{I,N-N,\beta'} P_{J,N,\beta-\beta'-1} \quad (107)$$

where

$$A_I = \frac{k_{pI}M}{\gamma_I} \quad (108)$$

$$L_{IJ} = \frac{k_{LCBI}}{\gamma_I} \frac{K_J}{k_{LCB1}P_1 + k_{LCB2}P_2 + s} \quad (109)$$

Equation 107 is a recursion relation that can be used to obtain the full distribution of  $P_{I,N,\beta}$  given the value of  $P_{I,1,0}$ . This is found, at steady state, to be

$$P_{I,1,0} = \frac{(K_I^s + K_I^-)P_I}{k_{pI}M + k_{LCBI}(D_1^- + D_2^-) + s} \quad (110)$$

Hence, given values of  $P_1$ ,  $P_2$ ,  $M$ ,  $k_{p1}$ ,  $k_{p2}$ ,  $k_{LCB1}$ ,  $k_{LCB2}$ ,  $K_1^-$ ,  $K_2^-$ ,  $K_1^s$ ,  $K_2^s$ , and  $s$  one can, by recursive application of (107), obtain the probability distribution of molecular weight and number of branches as

$$P(N,\beta) = \frac{P_{1,N,\beta} + P_{2,N,\beta} + D_{1,N,\beta}^- + D_{2,N,\beta}^- + D_{1,N,\beta}^s + D_{2,N,\beta}^s}{P_1 + P_2 + D_1^- + D_2^- + D_1^s + D_2^s} \quad (111)$$

## References and Notes

- (1) Lai, S. Y.; Wilson, J. R.; Knight, G. W.; Stevens, J. C.; Chum, P. W. S. US Patent 5,272,236 (Dow Chemical), 1993.
- (2) Lai, S. Y.; Wilson, J. R.; Knight, G. W.; Stevens, J. C. US Patent 5,665,800 (Dow Chemical), 1997.
- (3) Walter, P.; Trinkle, S.; Suhm, J.; Mäder, D.; Friedrich, C.; Mülhaupt, R.; *Macromol. Chem. Phys.* **2000**, *201*, 604.
- (4) Kokko, E.; Malmberg, A.; Lehmus, P.; Löfgren, B.; Seppälä, J. *J. Polym. Sci., Part A: Polym. Chem.* **2000**, *38*, 376.
- (5) Malmberg, A.; Liimatta, J.; Lehtinen, A.; Löfgren, B. *Macromolecules* **1999**, *32*, 6687.
- (6) Weng, W.; Markel, E. J.; Dekmezian, A. *Macromol. Rapid Commun.* **2000**, *21*, 1103.
- (7) Markel, E. J.; Weng, W.; Peacock, A. J.; Dekmezian, A. *Macromolecules* **2000**, *33*, 8541.
- (8) Shiono, T.; Azad, S. M.; Ikeda, T. *Macromolecules* **1999**, *32*, 5723.
- (9) Dekmezian, A. H.; Jiang, P.; Soares, J. B. P.; Garcia-Franco, C. A.; Weng, W.; Fruitwala, H.; Sun, T.; Sarzotti, D. M. *Macromolecules* **2002**, *35*, 9586.
- (10) Beigzadeh, D.; Soares, J. B. P.; Duever, T. A. *Macromol. Symp.* **2001**, *173*, 179.
- (11) Soares, J. B. P.; Hamielec, A. C. *Polymer* **1995**, *36*, 2257.
- (12) Soares, J. B. P.; Hamielec, A. C. *Macromol. Theory Simul.* **1996**, *5*, 547–572.
- (13) Soares, J. B. P.; Hamielec, A. C. *Macromol. Theory Simul.* **1997**, *6*, 591.
- (14) Yannoulakis, H.; Yiagopoulos, A.; Pladis, P.; Kiparissidis, C. *Macromolecules* **2000**, *33*, 2757.
- (15) Read, D. J.; McLeish, T. C. B. *Macromolecules* **2001**, *34*, 1928–1945.
- (16) Costeux, S.; Wood-Adams, P.; Beigzadeh, D. *Macromolecules* **2002**, *35*, 2514–2528.
- (17) Beigzadeh, D.; Soares, J. B. P.; Duever, T. A.; Hamielec, A. E. *Polym. React. Eng.* **1999**, *7*, 195.
- (18) Karol, F. J.; Wasserman, E. P.; Kao, S. C.; Brady, R. C. European Patent Application 94309546.3 (Union Carbide), 1994.
- (19) Beigzadeh, D.; Soares, J. B. P.; Duever, T. A. *Macromol. Rapid Commun.* **1999**, *20*, 541.
- (20) Beigzadeh, D.; Soares, J. B. P.; Hamielec, A. E. *J. Appl. Polym. Sci.* **1999**, *71*, 1753.
- (21) Beigzadeh, D.; Soares, J. B. P.; Hamielec, A. E. *Polym. React. Eng.* **1997**, *5*, 143.
- (22) Soares, J. B. P. *Macromol. Theory Simul.* **2002**, *11*, 184–198.
- (23) Simon, L. C.; Soares, J. B. P. *Macromol. Theory Simul.* **2002**, *11*, 222.
- (24) Costeux, S. *Macromolecules* **2003**, *36*, 4168–4187.
- (25) Beigzadeh, D. *Macromol. Theory Simul.* **2003**, *12*, 174–183.
- (26) Iedema, P. D.; Hoefsloot, H. C. J. *Macromolecules* **2003**, *36*, 6632–6644.
- (27) Nele, M.; Soares, J. B. P. *Macromol. Theory Simul.* **2002**, *11*, 939–943.
- (28) Beigzadeh, D. PhD Thesis, Department of Chemical Engineering, University of Waterloo, 2000.

MA030354L